Journal of Alloys and Compounds 615 (2014) S13–S17

Contents lists available at ScienceDirect

Journal of Alloys and Compounds

journal homepage: www.elsevier.com/locate/jalcom

Transient liquid phase bonding of carbon steel tubes using a Cu interlayer: Characterization and comparison with amorphous Fe–B–Si interlayer bonds

Nicolas Di Luozzo [a,b,*], Michel Boudard [b], Béatrice Doisneau [b], Marcelo Fontana [a], Bibiana Arcondo [a]

[a] Laboratorio de Sólidos Amorfos, INTECIN, Facultad de Ingeniería, Universidad de Buenos Aires – CONICET, Paseo Colón 850, C1063ACV Buenos Aires, Argentina
[b] Laboratoire des Matériaux et du Génie Physique (CNRS UMR 5628), Grenoble Institute of Technology, MINATEC, Grenoble Cedex 1, France

ARTICLE INFO

Article history:
Available online 1 December 2013

Keywords:
Transient liquid phase bonding process
Cu foil
Carbon steel
Microstructural characterization
Mechanical properties

ABSTRACT

In the present work the transient liquid phase bonding process was performed to join seamless carbon steel tubes using commercially pure Cu interlayers. The structural and mechanical characteristics of the resulting bonds are compared with those achieved using amorphous Fe–B–Si interlayers, under the same process parameters: a holding temperature of 1300 °C, a holding time of 7 min and an applied pressure of 5 MPa.

The joined tubes microstructures were characterized by direct observations – scanning electron microscopy – and diffraction techniques – electron backscatter diffraction. Chemical analysis was performed using electron probe microanalysis.

Whereas the amorphous Fe-B-Si interlayer leads to a completion of the bonding process over the whole bonding area, the bond performed using a Cu interlayer achieved the completion of the bonding process only partially. As the Cu is a cementite promoter, the amount of cementite coexisting with ferrite grains is higher in the joint region (JR) – corresponding to the higher concentration of Cu – as compared with the heat affected zone (HAZ) and the base metal (BM). An opposite effect is observed when using Fe-B-Si interlayers due to the fact that the cementite is unable to form in Si enriched zones – the microstructure at the JR presents only ferrite grains.

Tensile tests show that the joined tubes using Cu or Fe–B–Si interlayers failed away from the bond, at the HAZ, attaining almost the same ultimate tensile strength of the BM, in the as-received condition. Hardness profiles across the bonding zone are in agreement with the observed microstructures at the different zones of the bond region.

© 2013 Elsevier B.V. All rights reserved.

1. Introduction

The transient liquid phase bonding (TLPB) process [1] makes use of an interlayer to join metallic components. This interlayer – of specific chemical composition and with a lower melting point compared with that of the base metal (BM), is positioned in between the faying surfaces. Upon heating at the bonding temperature, above the melting point of the interlayer but below the melting point of the BM, the interlayer melts and interdiffusion between the new liquid phase and the BM takes place. This process leads to the increase of the melting point of the liquid, resulting in their solidification during the holding time at the bonding temperature, that is, an isothermal solidification is achieved.

This bonding process has found many applications, mainly joining Ni-based superalloys components [2]. Common interlayers for TLPB contain boron as a melting point depressant, which can diffuse rapidly as an interstitial in face-centred cubic transition metals [3]. Particularly, the most used are Ni–B–Si and Ni–Cr–B–Si amorphous foils. Their amorphous nature allows its manipulation thanks to its great toughness, despite its thickness (e.g. 25 μm). Moreover, as being Ni-based alloys, their chemical composition is well suited to match Ni-based components.

Several applications of the TLPB process for Fe-based components, particularly steels parts, were investigated [4–7]. Ni–B–Si and Ni–Cr–B–Si amorphous foils were used – as for Ni-based alloys, but also Fe-based ones were tested in order to match as much as possible the chemical composition of the BM, like Fe–B and Fe–B–Si amorphous foils. On the other hand, TLPB of duplex

* Corresponding author at. Laboratoire des Matériaux et du Génie Physique (CNRS UMR 5628), Grenoble Institute of Technology, MINATEC, Grenoble Cedex 1, France. Tel.: +33 0456529328.
E-mail address: nicolasdiluozzo@gmail.com (N. Di Luozzo).

0925-8388/$ - see front matter © 2013 Elsevier B.V. All rights reserved.
http://dx.doi.org/10.1016/j.jallcom.2013.11.165

stainless steel were successfully carried out using a commercially pure Cu interlayer [8], but an extremely careful preparation of the faying surfaces was needed.

We have evaluated in the present work a suitable industrial and commercially viable application of the TLPB process using a commercially pure Cu interlayer, and hot-rolled seamless low carbon steel tubes as BM – with their faying surfaces in the as-machined condition. Results regarding their microstructure and mechanical properties are compared with those obtained with Fe–B–Si amorphous foils.

2. Experimental

2.1. TPLB process

The materials used in this study are hot-rolled carbon seamless steel tubes EN 10297-1 Grade E235, as BM, and commercially pure Alfa Aesar® Cu foil and METGLAS® SA1 amorphous Fe–B–Si foil, as interlayers. Their chemical compositions are listed in Table 1 (for the Cu foil the missing balance, 0.02 wt%, corresponds to impurities).

The steel tubes have an outside diameter of 73 mm and a wall thickness of 9.5 mm. Both interlayers have a thickness of 25 μm.

The butted surfaces of the tubes – in the as-machined condition – with a roughness average (Ra) of 10.8 μm (7.5 mm evaluation length and 2.5 mm cut-off length), are aligned in contact with the interlayer and placed into the coil of an induction furnace under a controlled reducing (10% H_2 + 90% Ar) atmosphere. A uniaxial pressure of 5 MPa is applied during the bonding process. The temperature at the joint – measured on the outer surface of the tube by means of infrared thermometry at a sensing wavelength of 1600 nm, was raised to the process temperature (≈1300 °C), held constant for 7 min, and then cooled in still air to room temperature.

2.2. Microstructure characterization

2.2.1. Samples observations

Electron backscatter diffraction (EBSD) was used to obtain inverse pole figure (IPF) maps. Measurements were done in Zeiss Ultra 55 field-emission gun-scanning electron microscope (FEG-SEM), equipped with an EBSD detector EDAX DigiView III. The data was post-processed by means of EDAX OIM Analysis software. Step sizes from 0.25 to 2 μm were used for scanning, with an acceleration voltage of 20 kV.

Microstructure characterization was carried out with FEI Quanta 250 FEG-SEM, using an acceleration voltage of 15 kV.

Precise quantitative chemical analysis was performed by electron probe microanalysis (EPMA) with CAMECA SX50.

2.2.2. Samples preparation for microstructural characterization

The samples were cut perpendicularly to the joint along the longitudinal direction of the tubes. At first all the surfaces were grinded, mechanically polished with diamond suspension of 6 and 1 μm, and a different final stage was used depending on the particular surface sample required by the observation technique: 0.05 μm colloidal silica suspension was used for EBSD observations, 0.3 μm alumina suspension followed by 30 s etching with 2% Nital solution for FEG-SEM, and no final polishing nor etching for EPMA.

2.3. Mechanical properties characterization

Both tensile and hardness tests were used to characterize the mechanical properties of the joint and the BM.

The tensile tests were performed at a strain rate of 8 mm/min using samples cut both from the joined tubes and a tube in the as-received condition in accordance to ASTM E8M (5 mm thickness, 120 mm gauge length and 13 mm gauge width). Microindentation hardness profiles were carried out across the bonding zone using a 200 gf load at the joint region (JR) and a 1000 gf load at the heat affected zone (HAZ) and BM.

Table 1
Chemical composition (in wt%) for BM – E235 steel, and interlayers – SA1 and Cu.

	C	Mn	Si	S	P	B	Cu	Fe
E235 steel	0.12	1.09	0.24	0.0012	0.015	–	–	Balance
SA1			5			3	–	Balance
Cu foil							99.8	

3. Results and discussion

3.1. Microstructural characterization

3.1.1. Microstructure of the BM and the HAZ

Fig. 1a shows a prominent banded microstructure for the BM containing ferrite and pearlite. EBSD analysis shows that this microstructure consists of grains with an average diameter of 19 μm with a random orientation, characteristic of a fully recrystallized microstructure. This is intrinsic of the hot-rolling process applied to the BM, which involves a phase transformation after plastic deformation. Indeed the texture generated during rolling at high temperature is mostly removed when cooling by the subsequent phase transformation from austenite to ferrite.

When comparing the microstructure of the HAZ with that of the BM it appears that it is also containing ferrite and pearlite, but without any banded structure. The HAZ microstructure also reveals a grain growth process (Fig. 1b) with an average grain diameter of 38 μm as obtained from EBSD analysis.

3.1.2. Microstructure of the JR

3.1.2.1. Cu interlayer. The TLPB process was not systematically achieved at the JR – that is, the zone in which the microstructure was affected by the different stages of the TLPB process, but does not correspond to the microstructure of the HAZ. Two microstructures across the JR were observed depending on the completion or not of the process as seen in Fig. 2 (top panel):

- Yellow line (a) corresponds to a fully completion of the TLPB process. The microstructure presents ferrite and pearlite. EPMA chemical composition profile of Cu along the yellow line (a) (Fig. 2 (middle panel)) corresponds to a Cu enriched ferrite.
- Yellow line (b) corresponds to a partially achieved TLPB process. The microstructure presents, besides ferrite and pearlite, a Cu rich phase with white contrast corresponding to athermally solidified liquid (ASL), that is, the transient liquid phase which was unable to solidify isothermally. EPMA chemical composition profile of Cu along the yellow line (b) (Fig. 2 (bottom panel)) shows a Cu-rich ASL.

At the JR where the isothermal solidification was completed, grains of each side of the joint form HAGB, clearly separating each part of the bonded tubes (Fig. 3). Also the precise extent of the JR can only be determined in conjunction with chemical composition profiles and microstructural analysis. This is due to the fact that several grains of the JR have similar crystal orientations to that of the grains in the HAZ.

Along the JR, the pearlite/ferrite ratio is higher compared with the HAZ and BM, in accordance with literature, since Cu is a pearlite promoter [9] (Fig. 4).

3.1.2.2. Fe–B–Si interlayer. The completion of TLPB process was completely achieved at JR and its microstructure consists only of ferrite grains. This is directly related to the fact that Si prevents the formation of cementite [10], and a pearlite-free JR is obtained (Fig. 5a).

At the joint the bonded tubes are not separated only by grain boundaries but by a region – the JR. And the JR is, to a high extent, delimited by HAGB (Fig. 5b).

3.2. Mechanical properties

3.2.1. Tensile test

Samples bonded with a Cu interlayer, attained an ultimate tensile stress (UTS) of 489 MPa, achieving 95% of the UTS of the

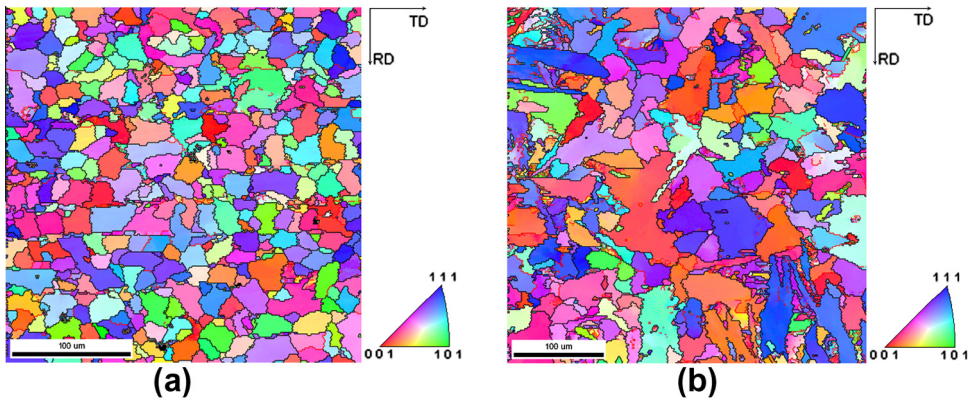

Fig. 1. Microstructure of the BM (a) and the HAZ (b): Normal direction (ND)-projected IPF map. Black lines denote high-angle grain boundaries (HAGB) – $\theta > 15°$, and red lines denote low angle grain boundaries (LAGB) – $\theta \leqslant 15°$. The rolling direction (RD) and the transverse direction (TD) are indicated on the figure. (For interpretation of the references to color in this figure legend, the reader is referred to the web version of this article.)

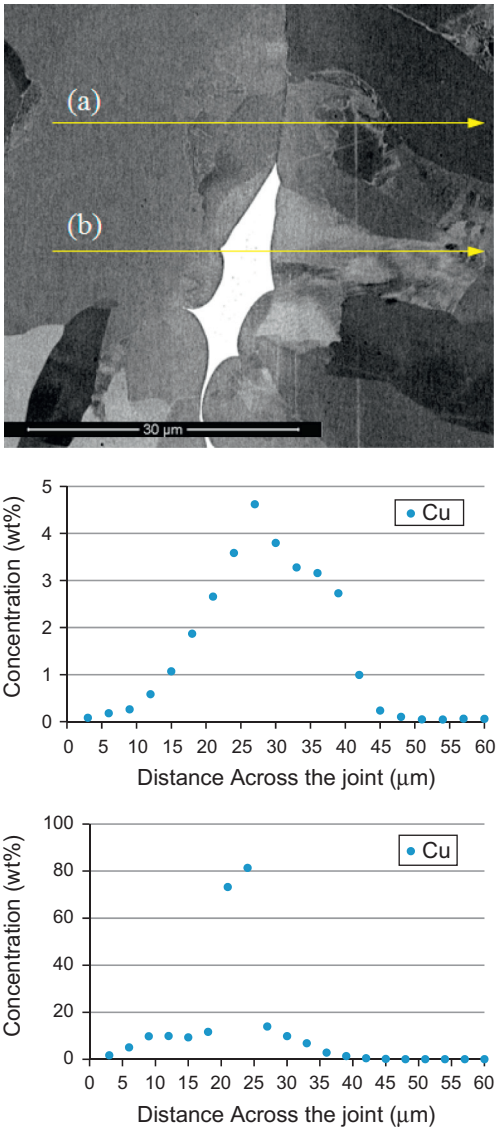

Fig. 2. Top panel: microstructure of the JR for the TLPB using a Cu interlayer as obtained by FEG-SEM (Back scattered electron mode). White contrast phase corresponds to ASL. The yellow lines indicate profile directions across the bonding corresponding to a complete (a) and incomplete (b) TLPB. EPMA Cu concentration profiles of Cu at the JR along (a) (middle panel) and (b) (bottom panel). (For interpretation of the references to color in this figure legend, the reader is referred to the web version of this article.)

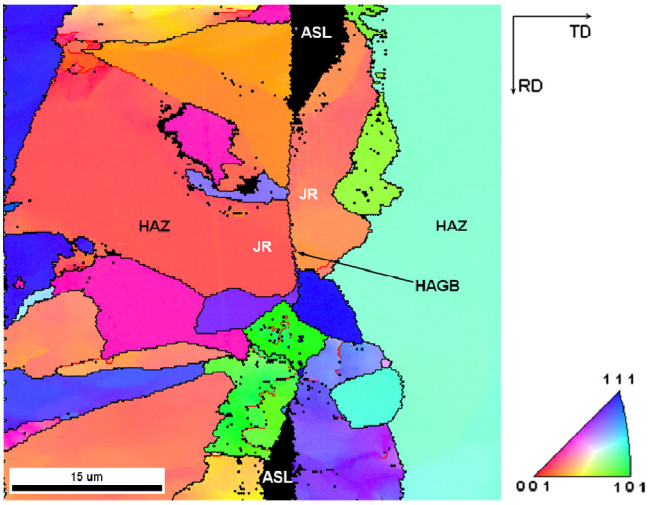

Fig. 3. ND-projected IPF map from the JR – Cu interlayer bond. In the map, black lines denote HAGB and red lines denote LAGB. The JR, HAZ and ASL are indicated on the figure.

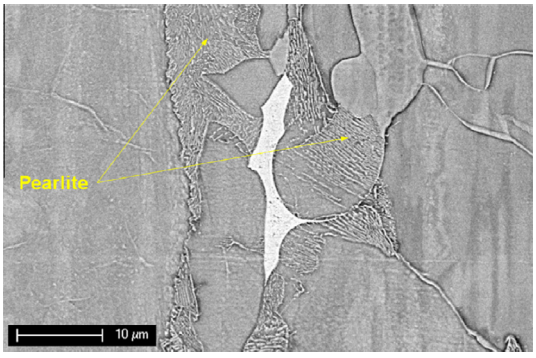

Fig. 4. FEG-SEM micrograph of Cu interlayer bond at the JR – backscattered secondary electrons. Pearlite colonies at the JR are indicated on the figure. White contrast phase corresponds to ASL.

BM in the as-received condition – 512 MPa, with failure occurring well away from the JR.

In the same way, amorphous Fe–B–Si interlayers bonded samples achieved 96% of the UTS of the BM, with failure occurring again well away from the JR.

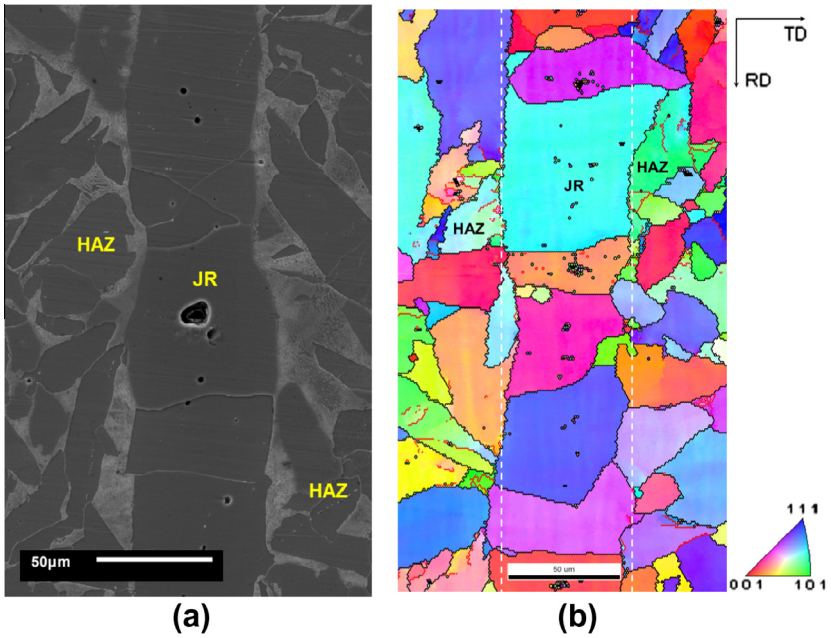

Fig. 5. Microstructure at the JR for Fe–B–Si interlayer – The JR and HAZ are indicated on the figures (a) FEG-SEM micrograph of the joint – secondary electrons and (b) IPF map. In the map, black lines denote HAGB and red lines denote LAGB. Also, the white dotted lines are a guide to the eye of the extension of the JR. (For interpretation of the references to color in this figure legend, the reader is referred to the web version of this article.)

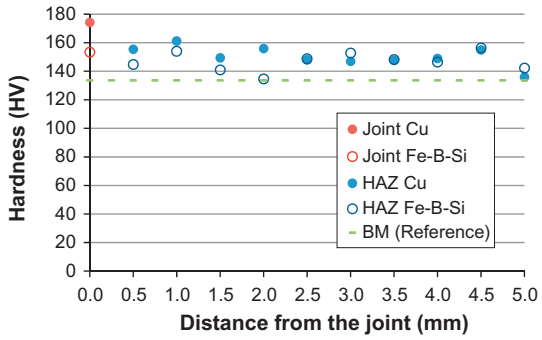

Fig. 6. Hardness distribution across the bonding zone.

In both cases, the small reduction of the UTS, compared with the BM, can be due to the deleterious effects of the TLPB thermal cycle, mainly the removal of the banded structure and grain growth.

3.2.2. Hardness profiles

Microindentation testing was carried out to display the hardness values at the joint. The hardness profiles of the bonded tubes, both using Cu – where the solidification process was completed – and Fe–B–Si interlayers, are shown in Fig. 6. The hardness both at the JR and at the HAZ next to the JR is slightly higher than that of the BM. This can be explained as follows:

- For Cu interlayers, the pearlite/ferrite fraction at the JR region is higher compared with the BM. Taking into account that the hardness of the pearlite is higher than that of the ferrite, it can be concluded directly that the JR must be a zone with increased hardness. On the other hand, for Fe–B–Si interlayers, the JR is enriched in Si, which is usually used to increase hardness [11].
- The cementite fraction at the HAZ next to the JR is slightly higher than that of the BM, leading to an increase in hardness. This is due to the fact that this zone was cooled to room temperature more rapidly than the whole tube after the hot-rolling process.

4. Conclusions

The TLPB was used to join low carbon hot-rolled seamless steel tubes using commercial grade Cu and amorphous Fe–B–Si foils as interlayers.

In both cases it was observed that at the HAZ, the almost fully recrystallized banded microstructure of the BM disappear and grain growth is observed.

When using Cu interlayers, the completion of TLPB process was not systematically achieved corresponding in the JR to the presence of zones with ASL, clearly distinct from the zones where the TLPB process was achieved. In these zones, HAGB clearly separates each part of the bonded tubes. Furthermore, several grains of JR are shared with the HAZ. Additionally, the pearlite/ferrite ratio at the JR was higher than those of the HAZ and the BM.

In comparison, when using Fe–B–Si interlayers, the completion of TLPB process was completely achieved at the JR and its microstructure consists only of ferrite grains, since Si prevents the formation of cementite. Also, the JR is, to a high extent, delimited by HAGB.

Tensile tests show that the joined tubes both using Cu and Fe–B–Si interlayers failed away from the bond, at the HAZ, attaining almost the ultimate tensile strength of the BM, in the as-received condition. Removal of the banded structure and grain growth are connected with the decrease of the UTS with respect to that of the BM.

The hardness profiles of the bonded tubes, both using Cu and Fe–B–Si interlayers, show that the hardness at the JR and at the HAZ next to the JR, is slightly higher than that of the BM, in agreement with the observed microstructures.

Notwithstanding their promising results, the uncompleted solidification stage of the samples bonded with Cu interlayers leads to the formation of the softer Cu-rich ASL. The presence of this

phase at the JR is detrimental to its mechanical properties and should be discarded in view of its industrial application. To overcome this difficulty and match the samples bonded with Fe–B–Si interlayers, the completion of the solidification stage must be assured, e.g.: increasing the isothermal holding time.

Acknowledgements

Financial support from the European Commission (Arcoiris Erasmus Mundus Scholarship) and from the FIUBA is gratefully acknowledged.

References

[1] I. Tuah-Poku, M. Dollar, T.B. Massalski, Metall. Trans. A 19 (1988) 675–686, http://dx.doi.org/10.1007/BF02649282.
[2] S. Duvall, W.A. Owczarski, D.F. Paulonis, Weld. J. 204 (1974) 203–214.
[3] W.F. Gale, D.A. Butts, Sci. Technol. Weld. Join. 9 (2004) 283–300, http://dx.doi.org/10.1179/136217104225021724.
[4] S. Kishi, T. Maenosono, M. Sato, US Patent 5875954, 1999.
[5] Y. Hamada, Y. Fukada, M. Ueda, Y. Komizo, US Patent 6059175, 2000.
[6] T. Shimizu, H. Horio, K. Kito, S. Inagaki, R. Yamada, US Patent 6592154 B2, 2003.
[7] N. Di Luozzo, M. Fontana, B. Arcondo, J. Mater. Sci. 43 (2008) 4938–4944, http://dx.doi.org/10.1007/s10853-008-2720-0.
[8] T.I. Khan, M.J. Kabir, R. Bulpett, Mater. Sci. Eng. A (2004) 290–295, http://dx.doi.org/10.1016/j.msea.2004.01.023.
[9] R.A. Gonzaga, Mater. Sci. Eng. A (2013) 1–8, http://dx.doi.org/10.1016/j.msea.2012.12.089.
[10] H. Bhadeshia, R. Honeycombe, Steels: Microstructure and Properties, Elsevier, Amsterdam, 2006.
[11] B.L. Bramfitt, A.O. Benscoter, Metallographer's Guide: Practices and Procedures for Irons and Steels, ASM International, Novelty, 2002.